Experimentální Analýza Napětí 2009
Experimental Stress Analysis

INNOVATIVE METHODS IN THE FIELD OF DEFORMATION ANALYSIS

Aleš Volek[1]

Abstract: In fact, the development costs in the industry raise a lot nowadays. Because of it, it is important to use new innovative and cost-reducing development methods. It is not useful to produce the prototypes for all range of problems, considering the expensive price. Instead of this, it is more suitable to use long-range simulations for complex movement and deformation procedures. Using simulations, optimization of detailed constructions is possible and due to this, reductions in the development time and a minimilization of development iterations is caused. But even if the simulations results are correct, they need to be confirmed in tests and the maximum load of components should be verified. For this purpose, non-contact, optical measuring systems are used. The process of using cameras for capturing the coordinates respectively the position and displacement of measuring position can give a large advantage to traditional measuring techniques use electronic sensors by reducing the measuring time. The fast adaptation to new measurement setups and the multitude of easy to apply 3D measurement points allow a precise and efficient strain analysis. Furthermore, optical measurement methods enable a visual presentation of measurement results, which makes a result interpretation easy and intuitive. Examples of new optical measurement systems will be given.

1. Introduction

There are many principles describing optical techniques for deformation measurements [1], [2]. The following text will be focused on the principle of photogrammetry and image correlation. Both of them are widely used by optical measurement system and therefore it is necessary to obtain the basic details, which can be used to understand those systems in general.

2. Image Correlation

2.1. Principle of Image Correlation

The process of image correlation is actually very simple. The measuring object (specimen) is covered by stochastic pattern which is usually done by splashing white spray as a background while the black spray is distributed just partially. Then, the specimen is put under the load and the images of measuring area are recorded continuously. Wide range of CMOS cameras are in use, depending on measuring frequency or camera resolution. After the loading is finished and the images are recorded simultaneously by two cameras, the software correlation solution comes into play The software solution divides the measurement area into small semi-areas, in which the specific number of white and black pixels is counted *(“grey index”) (Figure 1, Figure 2).* The fact that the pattern was made by hand to ensure that the *grey index* is a unique number and is not repeated in the whole area. In the very next stage, the position of the same area is investigating according to the *grey index (Figure 3, Figure 4).* This workflow is done for all overlapped areas in all stages resulting in a nice overview of the whole measurement area. The following examples were created by using the image correlation system ARAMIS[2].

[1] Ing. Aleš Volek; MCAE Systems; Knínická 1771, 664 36 Kuřim, Czech Republic, ales.volek@mcae.cz
[2] GOM mbH., Mittelweg 7-8, 38106 Braunschweig, Germany, www.gom.com

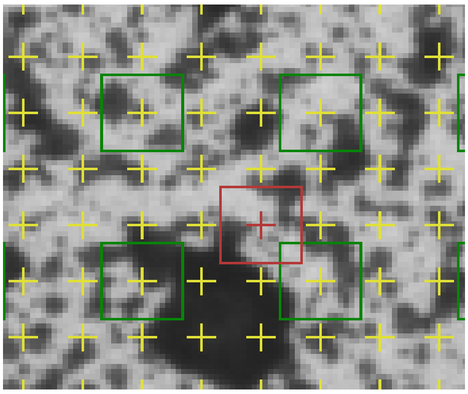

Figure 1. *Non-deformed stage – Left camera*

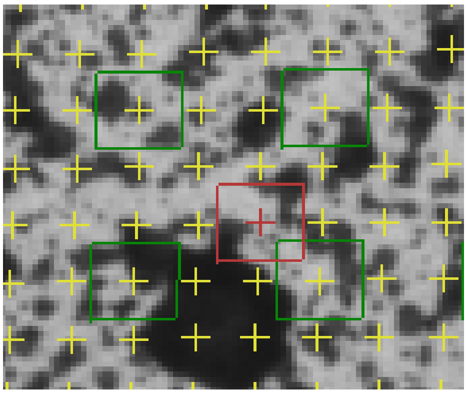

Figure 2. *Non-deformed stage –Right camera*

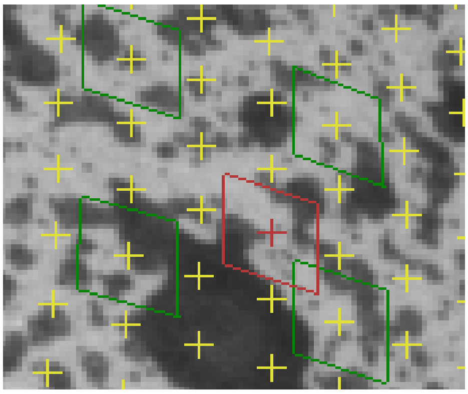

Figure 3. *Deformed stage – Left camera*

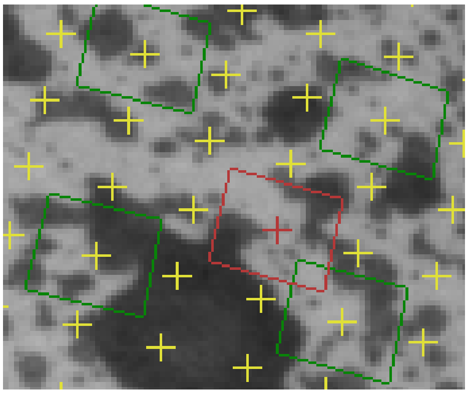

Figure 4. *Deformed stage –Right camera*

2.2. Practical use of image correlation

Determining the Yield Stress During a Tensile Test [3]

The tensile test specified in DIN EN 10002-1 determines the material characteristics using strongly defined specimen geometry and very tight test parameters. During the test, the active force, the strain and the cross-section are measured continuously. The strain is integrated via the measuring length of the strain gauge (usually 50 or 80 mm). The specific stress corresponds to the active force divided by the cross-section of the specimen in the measuring range. The change in the cross-section during the test is calculated from the longitudinal strain of the specimen (constant volume $A_0l_0 = A_nl_n$).

After reaching the uniform strain, the local necking of the specimen starts. At this point, the determination of the specimen's cross-section becomes incorrect when using a conventional tactile strain gauge as the longitudinal change of the specimen is averaged over the entire measuring length. The strongly increased local strain values and their changes in space and time are therefore not captured with the standardized tensile test.

Using the ARAMIS system, however, allows for determining the local deformations in both surface directions for a defined surface and, based on the consistent volume, for calculating the thickness reduction as well. This gives additional information about the uniform and non-uniform distribution of the spatial and temporal deformations on the surface of the specimen. The necking area can be investigated in more detail and the local changes in the cross-section of the necking area and its environment can be determined. In addition, Lüders bands occurring locally and their changes are measurable and graphically visualized during the tensile test.

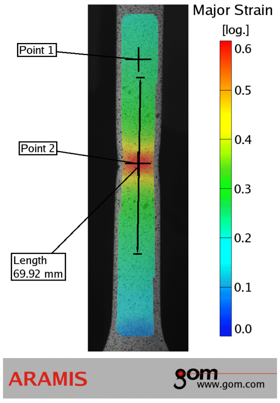

Figure 5. *Local measuring values with drawn in measuring length of common strain gauges*

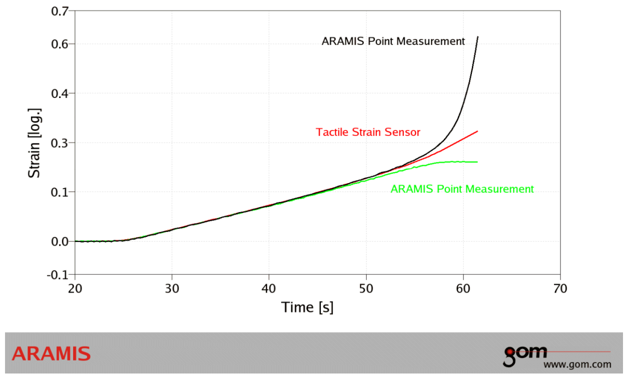

Figure 6. *Local ARAMIS measuring values in the necking area and far away from the necking compared to "averaged" tactile measuring values*

Figure 5 shows the "local" strain recorded with ARAMIS, in this case the major strain, together with the "global" measuring value of a tactile strain gauge for the same specimen. The local strain values are available for each point of the tested surface for the entire duration of the measurement.

Figure 6 shows the global strain characteristic determined by a tactile strain gauge in the tensile test as a function of time. This strain characteristic is compared to the strain characteristic locally measured with ARAMIS in the necking area.

For small deformations, the measuring values match well. Just before breaking, the local strain in the necking area (ARAMIS measuring values, black line) deviates from the global value measured with the tactile strain gauge. As the strain gauge integrates the strain over its entire measuring length (red line) it cannot provide local peak values. As soon as the necking starts, the deformation of the specimen concentrates more and more in the necking area (black line). Areas far away from the necking deform less and less and just before breaking they no longer deform at all (green line). In order to achieve a local measuring value (high measuring data density at short basic length), using the optical measuring system ARAMIS is recommended. The complete deformation behavior of the specimen can be captured and evaluated during the deformation process up to the moment of breaking by recording and evaluating numerous stereo image pairs (synchronous recording of both cameras) together with the corresponding load values (force).

Determining of Process Limitations in Sheet Metal Forming [4]
Forming Limit Diagram (FLD)

The Forming Limit Diagram (FLD) together with the Forming Limit Curve (FLC) provide a method for determining process limitations in sheet metal forming and are used to assess the stamping characteristics of sheet metal materials. Usually, the Forming Limit Diagram is used in method planning, tool manufacturing and in tool shops to optimize stamping tools and their geometries. The comparison of deformations on stamped metal sheets using the FLD leads to a security estimation of the stamping process. The forming analysis and the comparison of the data with the FLC provide for a reliable assessment of sheet metal forming processes.

Normally, the material manufacturer determines the Forming Limit Curves according to the Nakajima or Marciniak tests. This way, the material quality can be clearly defined, which helps the customer to choose the right material.

Determination of Forming Limit Diagrams According to Nakajima [4]

The Nakajima test is based on the principle of deforming sheet metal blanks of different geometries using a hemispherical punch until a fracture occurs (Figure 7). By varying the specimen width (Figure 8), different deep draw and stretch forming conditions occur on the sheet metal surface (from a regular biaxial deformation to a simple tensile load). The characteristic, maximally achievable deformations (prior to breakage) of the different specimen shapes are determined and define the forming limit curve of the corresponding material. So far, a forming limit curve was generally determined by applying a pattern of circles and lines to the sheet metal blanks prior to the forming process. Due to the load on the sheet metal, these circular marks deform to ellipses, the main axes of which represent the strain on the surface in major and minor direction. After the forming process, the "deformed" line patterns were measured manually using measuring magnifying glasses, microscopes and flexible measuring strips. This method is limited by the contour sharpness of the deformed pattern, the time-consuming evaluation, the low local resolution and the subjective, user-dependent recording of measurement values.

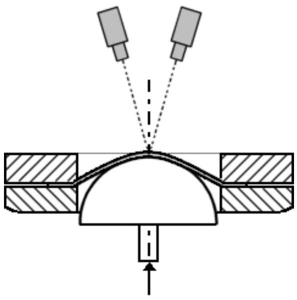

Figure 7. *Test arrangement according to Nakajima*

Figure 8. *Different specimen geometries, from the entire blank to strongly waisted blanks*

In order to meet today's requirements, the characteristics of sheet metal materials must be determined precisely, reproducibly and efficiently. By using the optical measurement system ARAMIS, the preparation of the specimens, the forming process and the determination of the deformation characteristics can easily and reproducibly be carried out such that today exact material characteristics are available at low costs.

When preparing the specimens, a stochastic pattern is applied to the surface using a color spray (Figure 9), instead of the circular or line mesh. In addition, guidelines were prepared (according. to ISO 12004 Recommendation) which guarantee a regular and reproducible load of the specimen.

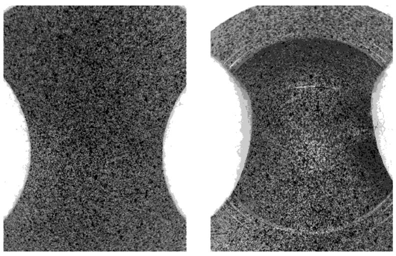

Figure 9. *Non-deformed and deformed Nakajima specimens with stochastic pattern*

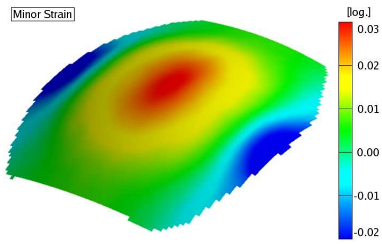

Figure 10. *Minor strain, punch dome area*

Recording of the line mesh is replaced by the allocation of stochastic patterns. Thus, the number of measuring points is considerably increased. In addition, minor blurs and defects in the pattern are compensated such that numerous reliable measuring values are created.

ARAMIS automatically divides the reference image into small overlapping areas (squares or rectangles) and defines the corresponding area in the stereo image. Optimized calculation methods provide for assigning the corresponding area ultra-precisely (sub pixel range). By assigning all image details to the stereo image, the shape of the sheet metal in its reference state is measured based on the calibration data of the system. Now, the image details of the reference image can be allocated to the images of the recorded subsequent stereo image pairs. Thus, after the automatic evaluation, the shape and the deformation of the sheet metal was precisely recorded and measured for each recording moment. Anyway, for a fast

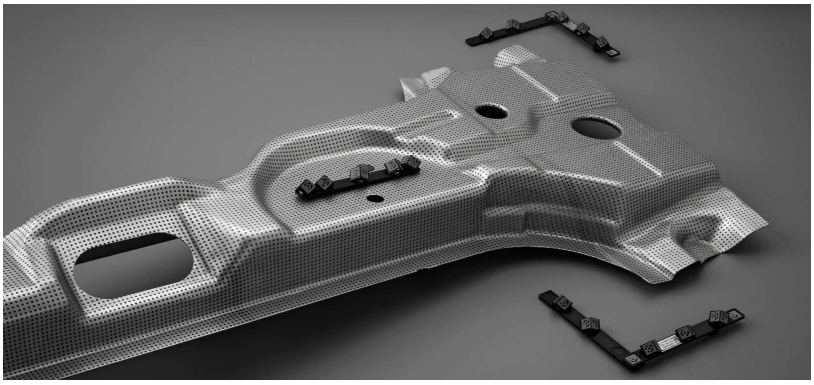

Figure 13. *Stamped part with point pattern and special markers*

calculation of the points on the Forming Limit Curve, sometimes only the reference image pair before applying the load and the last image pair directly before the fracture occurs are evaluated. This guarantees that heavily loaded areas are captured and included into the FLC determination.

In the ARAMIS software, sections are defined perpendicular to the break line to calculate the FLC data. From this section data (normally five parallel sections) a FLC point with its measuring deviation is calculated automatically according to the currently valid guidelines. For customized FLC calculations, this section data can be exported and processed using proprietary evaluation algorithms. The measuring values are shown as 3D section graphics (Figure 11) and in a Forming Limit Diagram (Figure 12). ARAMIS calculates the characteristic values (theoretical maximum of major and minor strain) by the computation of an ideal shape of the curve from the captured measuring values. Figure 12 shows the measuring results of eight different sheet metal geometries. For each geometry, the deformations at material failure were evaluated for three specimens each with three sections and displayed in the FLD diagram.

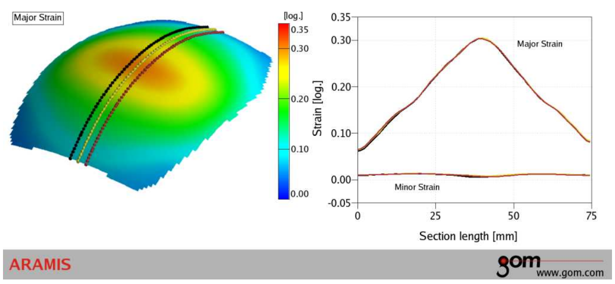

Figure 11. *Sections with respective section data. The diagram shows the major and the minor strain over the section length*

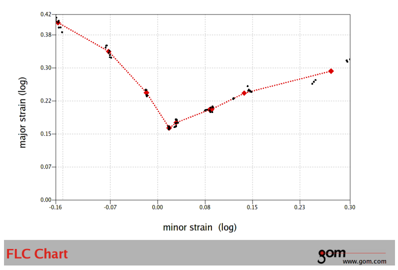

Figure 12. *FLC of a 1 mm thick steel sheet metal*

Result Combination of More Systems [5]

The result shown at Figure 12 can be immediately used in combination with another optical measuring system ARGUS[1], which is designed to measure the strain and thickness reduction in sheet metal caused by stamping, to detect hot spots in the validation process of new and reworked stamping tools, and to measure the formability of sheet metal in stamping applications.

To begin the part to be measured must be covered with special kind of dots pattern before the deformation (Figure 13). These dots are made by an electrochemical way, or using the laser. After the stamping process, several pictures of the part including some special markers are taken. This is done by high resolution camera and the 3D coordinates of each dot are computed. The change of distances of the neighboring points defines the strain in this area of the part. With the assumption that the point pattern moves in accordance with the material and the sheet is thinned, the reduction of the thickness of the part due to the deformation is displayed in Figure 14. The corresponding Forming Limit Diagram (FLD) in Figure 15.

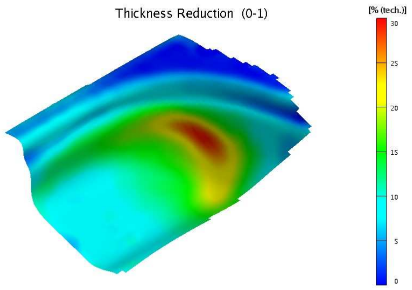

Figure 14. Reduction of the sheet thickness

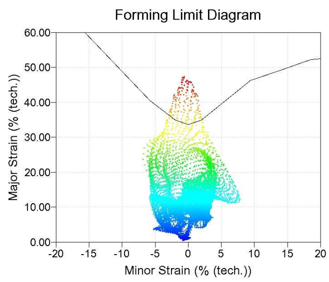

Figure 15. *Corresponding FLD*

The FLD shows clearly that many measurement points are above the forming limit curve of the used material. In these areas the part will probably tear or is so weak that it can not be used at all. Using the additional information given by ARGUS (flow direction, display of the non-deformed sheet with its expected reduction in thickness, major and minor strain) the tool was reworked and the stamping parameters were adapted. A new measurement was performed in some minutes to verify the changes.

In Figure 16, the results of the second ARGUS measurement are shown, from a stamping test using the modified tool and adapted stamping parameters.. Displayed is the form after stamping, with color coded display of the thickness reduction of the sheet due to stamping. The corresponding FLD of all measured points is also displayed in Figure 17. The image shows that the stamping process is well in tolerance in this area.

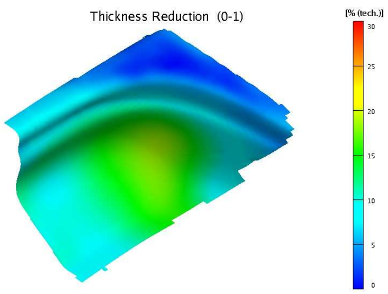

Figure 16. *Resulting thickness after modification*

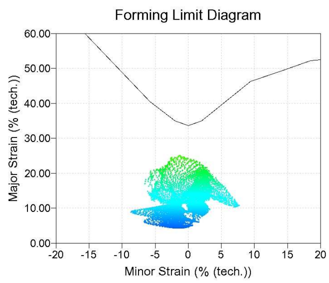

Figure 17. *Corresponding FLD after modification*

3. Photogrammetry

3.1. Principle of photogrammetry

The roots of photogrammetry can be found at the beginning with photography. The principles were developing during 20th century and are described in many sources [6], [7]. Therefore, just an overlook to the applications example will be given and two optical measuring systems (PONTOS[1] and TRITOP[1]) will be described.

3.2. Practical use of photogrammetry

Both PONTOS and TRITOP use the principle of triangulation [6] which enables a precise 3D coordinates determination of measuring markers (unlimited number of paper or magnetic stickers). While PONTOS uses two high-speed CMOS cameras, TRITOP uses just one hand-held high-resolution camera (for example, a Canon EOS 1Ds Mark III). Therefore the TRITOP system is used for static or quasi-static actions and PONTOS for fast, dynamic actions.

Figure 18. *PONTOS cameras*

Figure 19. *TRITOP camera*

Depending on the cameras used, the measuring frequency can reach 50kHz or more, which is quite enough to register even very fast actions, such as a gun shot etc. Other PONTOS measurements examples are shown in Figure 20, Figure 21, and TRITOP measurement examples in Figure 22, Figure 23.

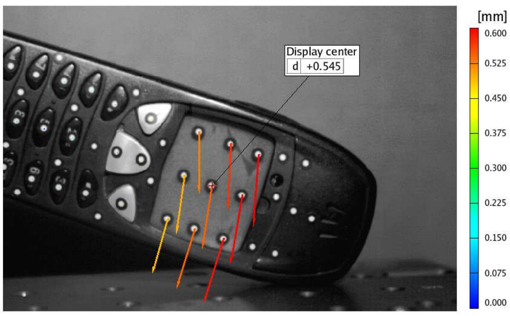

Figure 20. *Drop test of cell phone (7000Hz)*

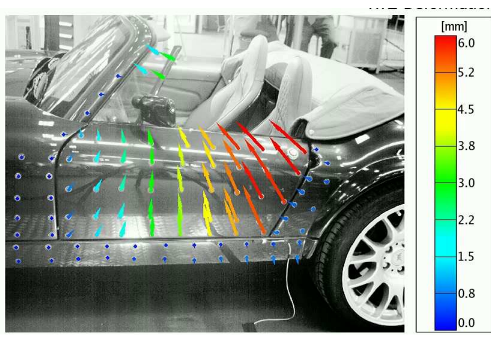

Figure 21. *Door slam (480Hz)*

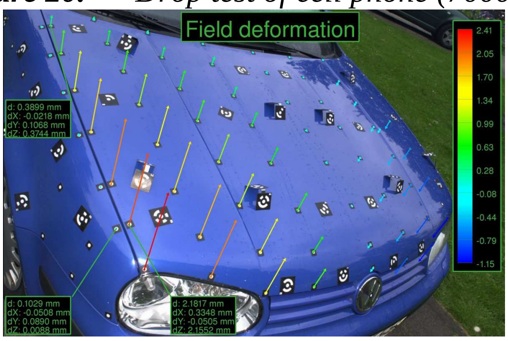

Figure 22. *Deformation of a car bonnet*

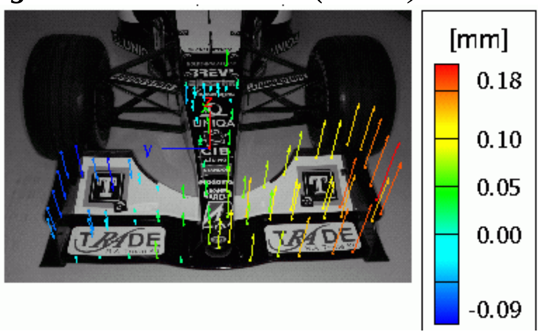

Figure 23. *Deformation after loading*

4. Conclusion

New ways on field of deformation analysis were shown and four optical measurement systems were presented. All of these systems can successfully be combined and the range of their application can be increased. The data and results are transferable between the software solutions, so examination of a large object from “component-testing-point-of-view” (PONTOS/TRITOP) with a “detailed view on surface behavior” (ARAMIS) is possible. All results can be visualized in one report, which caused that the deformation and stress analysis is much more comfortable.

References

[1] Williams, D.C, Ed., Optical Methods in Engineering Metrology, ISBN: 0412396408 Chapman and Hall, London & New York, 1993.

[2] Cloud, Gary, *Optical Methods of Engineering Analysis*, ISBN-10: 052145087X,Cambridge University Press, 1995.

[3] Gesellschaft für Optische Messtechnik, Mittelweg 7-8, Braunschweig, Germany, [Online: 5.3.2009], URL: <http://www.gom.com/EN/D2538E9425035D75C1257126004E05E6_B59F3B6E71DEB21EC1257107003CF424.html>

[4] Gesellschaft für Optische Messtechnik, Mittelweg 7-8, Braunschweig, Germany, [Online 5.3.2009], URL: <http://www.gom.com/EN/8933502D3837CB09C1257126004D55BC_B59F3B6E71DEB21EC1257107003CF424.html>

[5] Gesellschaft für Optische Messtechnik, Mittelweg 7-8, Braunschweig, Germany, [Online 5.3.2009], URL: <http://www.gom.com/EN/FE6F4BA356B86AAAC125711400347D7E_F43B506C9B252F11C12571220060A02C.html>

[6] THOMAS LUHMAN, *Nahbereichsphotogrammetrie* (2. release), ISBN: 3-87907-398-9 Heidelberg: Herbert Wichmann Verlag, 2003.

[7] Werner Bösemann, *Advances in photogrammetric measurement solutions*, Computers in Industry 56 (2005) 886–893.p